J. Fluid Mech. (1974), *vol.* 66, *part* 4, *pp.* 657–671
Printed in Great Britain

Steady flow in rapidly rotating circular expansions

By J. S. WALKER
Department of Theoretical and Applied Mechanics, University of Illinois, Urbana

(Received 18 January 1974 and in revised form 9 May 1974)

Inertialess incompressible flow through a rapidly rotating, variable-area conduit of circular cross-section is treated. For the practical case of an expansion (or contraction) placed between two pipes, the flow is strongly asymmetrical and involves regions of weak reverse flow in the expansion and downstream pipe, while the disturbance to the fully developed pipe flows persists for large, $O(E^{-\frac{1}{2}})$ distances upstream and downstream, where E is the (small) Ekman number. The flow in the two pipes depends only on the ratio of their radii and is independent of the shape and length of the expansion. The startling implication of the disturbance's persistence is that, in practice, fully developed flow will almost never be realized in rapidly rotating pipes.

1. Introduction

This paper treats the flow of a liquid through a circular expansion (or contraction) which is rotating rapidly about an axis perpendicular to its centre-line. The expansion's wall is defined by

$$y^2+z^2=f^2(x)$$

in a rotating co-ordinate system with the x axis along the centre-line and the y axis parallel to the axis of rotation (see figure 1). The flow is steady in this co-ordinate system. The speed of rotation is sufficiently great for inertia to be neglected and for viscous effects to be confined to thin boundary layers adjacent to the wall. The wall is assumed to be smooth (i.e. the slope f' is bounded and continuous), so that free shear layers parallel to the axis of rotation do not occur.

The most general solution of the inviscid core equations and boundary conditions at the wall is presented in § 2. The geometry of the entire conduit must be specified before the integration function in this solution can be determined.

For definiteness and because of its practical importance, an expansion placed between two semi-infinite pipes of different (constant) radii is considered in § 3. The problem is reduced to determining very slow changes in the flow over large, $O(E^{-\frac{1}{2}})$ lengths of the two pipes, where E is the (small) Ekman number. The analysis in each pipe is reduced to a single Sturm–Liouville eigenvalue problem. Once the eigenvalues and eigenfunctions have been found, the solution in each pipe can be written as an eigenfunction expansion, where the coefficients in the two expansions are determined by conditions linking the two solutions. A numerical procedure for finding the eigenvalues and eigenfunctions and the coefficients in the two expansions is given in § 4.

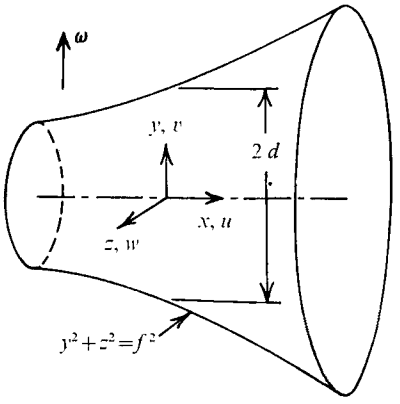

FIGURE 1. Expansion with circular cross-section.

The results for a conduit in which the radius of the downstream pipe is one and a half times that of the upstream pipe are presented in §5. The numerical values in the following general description refer to this conduit. The flow begins to deviate from fully developed flow at a distance $0{\cdot}25E^{-\frac{1}{2}}d$ upstream of the expansion, where d is the radius of the upstream pipe. The flow inside the expansion is geostrophic. The flow from the upstream pipe to the downstream one is split into a weak flow along the geostrophic surfaces in $-f < z < -(f^2-1)^{\frac{1}{2}}$ and a strong flow along those in $(f^2-1)^{\frac{1}{2}} < z < f$, while a weak flow along the surfaces in $|z| < (f^2-1)^{\frac{1}{2}}$ enters the expansion from and returns to the downstream pipe. In the downstream pipe, the flow returns to fully developed flow at a distance $0{\cdot}9E^{-\frac{1}{2}}d$ from the expansion. The flow in the two pipes is independent of y and of the shape f and length ld of the expansion.

The analysis presented here is similar to that given by Walker & Ludford (1974) for MHD flow in insulated circular expansions with strong transverse magnetic fields. Wherever possible the presentation here parallels that in Walker & Ludford's paper in order to emphasize the analogy between MHD and rotating flows.

2. Geostrophic flow

The flow considered here is incompressible and steady relative to a Cartesian co-ordinate system rotating at a constant angular velocity $\boldsymbol{\omega} = \omega\hat{\mathbf{y}}$ with respect to some inertial system, so that the non-dimensional governing equations are

$$\nabla.\mathbf{v} = 0, \quad Ro(\mathbf{v}.\nabla)\mathbf{v} = -\nabla\Phi - \hat{\mathbf{y}}\times\mathbf{v} + E\nabla^2\mathbf{v}, \tag{1a, b}$$

where

$$\Phi = (p/\rho + \phi - \tfrac{1}{2}\omega^2a^2)/2\omega Ud$$

is the reduced pressure (see Greenspan 1968, p. 6). Here $\hat{\mathbf{y}}$ is a unit vector in the y direction, $\mathbf{v}$ is the velocity, $Ro = U/2\omega d$ and $E = \nu/2\omega d^2$ are the Rossby and Ekman numbers respectively, p is the true pressure, ρ is the density, ϕ is the gravitational potential, a is the perpendicular distance from the axis of rotation, U is the characteristic velocity, d is the characteristic length and ν is the (constant) kinematic viscosity.

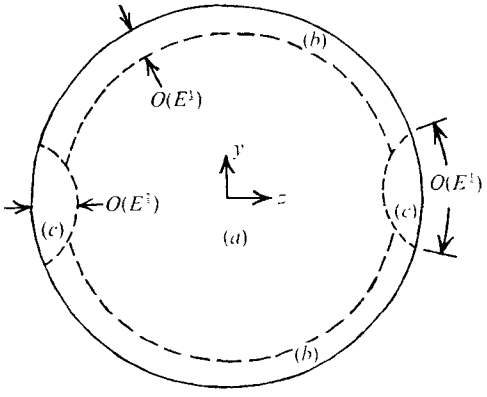

FIGURE 2. Cross-section showing flow subregions.

The flow is confined by an expansion (or contraction) with circular cross-sections and with its centre-line perpendicular to the axis of rotation (see figure 1). The radius at some section, say $x = 0$, is used for d, and the average velocity at the same section is used for U, so that

$$f(0) = 1, \quad \int_{-1}^{1} \int_{-(1-z^2)^{\frac{1}{2}}}^{(1-z^2)^{\frac{1}{2}}} u(0, y, z)\, dy dz = \pi. \tag{2a, b}$$

The boundary conditions are

$$\mathbf{v} = 0 \quad \text{at} \quad y = \pm (f^2 - z^2)^{\frac{1}{2}}.$$

Together with the governing equations (1) these form a homogeneous boundary-value problem whose solution is normalized by the mass-flux condition (2*b*).

For a sufficiently rapid speed of rotation the condition $Ro \ll 1$ holds, so that the inertia term on the left-hand side of (1*b*) can be neglected (see §6). If the condition $E \ll 1$ also holds the flow region can be divided into several parts, certain viscous terms in (1*b*) being negligible in each subregion. The various subregions (shown in figure 2) are (*a*) the core, (*b*) Ekman layers and (*c*) side regions.

The variables in the Ekman layers are determined locally by the tangential velocity outside and automatically match the core variables provided that the latter satisfy

$$ff'u = yv + zw \quad \text{at} \quad y = \pm (f^2 - z^2)^{\frac{1}{2}} \tag{3}$$

when $O(E^{\frac{1}{2}})$ terms are neglected. In other words, the no-slip condition at the wall is relaxed for the inviscid core flow since the viscous Ekman layers are able to satisfy the neglected no-slip condition and match the tangential core velocity outside. The Ekman layers break down near the points where the wall is parallel to the axis of rotation and side regions are needed to match the core variables near $y = 0$ as $z \to \pm f$ and the Ekman-layer variables near

$$y = \pm (f^2 - z^2)^{\frac{1}{2}}$$

as $z \to \pm f$.

Stewartson (1966) treated similar side regions and his analysis shows that the $O(1)$ solution elsewhere can be determined without considering the corner regions in detail as long as the core variables satisfy the regularity conditions

$$(f^2-z^2)^{-\frac{1}{4}}(u \pm f'w) \to 0 \quad \text{as} \quad z \to \pm f \quad \text{at} \quad y = 0, \tag{4}$$

which select the least-singular solution.

The core variables satisfying (1) and the Ekman conditions (3) are

$$u = \partial\Phi/\partial z, \quad v = 0, \quad w = -\partial\Phi/\partial x, \tag{5a, b, c}$$

where Φ is a function of $s = (f^2-z^2)^{\frac{1}{2}}$ alone and u, v, w and Φ now denote the $O(1)$ terms in the asymptotic expansions of the core variables (see §6). Vertical lines of fixed length $2c$ inside the expansion generate a geostrophic surface on which $s = c$, Φ is constant and $\mathbf{v}$ is horizontal and tangential. Thus the governing equations (1) and Ekman conditions (3) require the core flow to be geostrophic but do not specify how the total mass flux is distributed among the geostrophic surfaces.

For fully developed flow in constant-area pipes, Benton & Boyer (1966) extended the Ekman-layer solution to higher-order terms in order to obtain boundary conditions on the $O(E^{\frac{1}{2}})$ core variables at the wall. Together with the regularity conditions (4) these determined an integration function $\Phi(z)$ in their $O(1)$ core solution, as well as the $O(E^{\frac{1}{2}})$ y and z velocities, but left an integration function $\hat{\Phi}(z)$ in the $O(E^{\frac{1}{2}})$ reduced pressure with the $O(E^{\frac{1}{2}})$ x velocity $\hat{u}$ related to this function by $(5a)$ with carets added. In the present problem a higher-order Ekman-layer analysis yields no further conditions on the $O(1)$ solution (5) as long as $f' \neq 0$. However, when $f' = 0$ and $\partial/\partial x = O(E^{\frac{1}{2}})$, the relationship between the terms in the governing equations (1) and Ekman conditions changes, so that the solution (5) is not the correct one and the situation is similar to that for fully developed flow. Therefore, in order to determine the function $\Phi(s)$ for a given expansion, the geostrophic surfaces must be followed until they enter a constant-area pipe in which the flow is changing slowly.

3. Expansion between two pipes

For definiteness an expansion placed between a pair of semi-infinite pipes with different (constant) radii is considered, so that

$$f = \begin{cases} 1 & \text{for} \quad x \leqslant 0, \\ e & \text{for} \quad x \geqslant l, \end{cases}$$

where the expansion ratio $e > 1$. For a contraction placed between two pipes, the geometry is reversed,

$$f = \begin{cases} e & \text{for} \quad x \leqslant -l, \\ 1 & \text{for} \quad x \geqslant 0, \end{cases}$$

and the solution is obtained by changing the signs of certain variables in the solution for an expansion. For a smooth expansion $f'(0^+) = f'(l^-) = 0$.

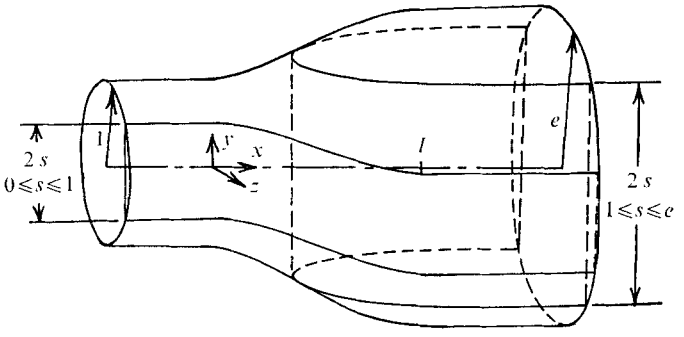

FIGURE 3. Geostrophic surfaces $s = (f^2(x) - z^2)^{\frac{1}{2}}$.

Two typical geostrophic surfaces in an expansion are sketched in figure 3. The surfaces for $0 \leqslant s \leqslant 1$ extend from $x = -\infty$ to $x = +\infty$, while those for $1 < s < e$ begin and end at $x = +\infty$. If the solution (5) held everywhere, then whatever the flow upstream, it would be carried into two separated regions $(e^2-1)^{\frac{1}{2}} < |z| < e$ downstream, while the flow in between $[|z| < (e^2-1)^{\frac{1}{2}}]$ would have an x velocity profile antisymmetric in z. This hypothetical flow in the downstream pipe satisfies the condition for fully developed flow, i.e. $\partial/\partial x = 0$, but it is clearly not the flow found by Benton & Boyer (1966). The contradiction arises because gradual changes occurring over large, $O(E^{-\frac{1}{2}})$ distances in both pipes have been ignored. The Ekman conditions (3) and thus the solution (5) neglect $O(E^{\frac{1}{2}})$ velocities, but over an $O(E^{-\frac{1}{2}})$ length of pipe, such a velocity normal to the geostrophic surfaces can account for a slow migration of the flow across these surfaces. It turns out that this slow migration allows the flow to become fully developed as $E^{\frac{1}{2}}x \to +\infty$, but also causes the flow to deviate from fully developed by an $O(E^{-\frac{1}{2}})$ distance upstream of the expansion.

In order to study the slowly evolving flow in both pipes, the x scale is compressed by introducing a new co-ordinate

$$X = E^{\frac{1}{2}}x.$$

The expansion now collapses onto the plane $X = 0$, and the problem is reduced to finding an outer solution for the upstream pipe ($X < 0$) and another for the downstream pipe ($X > 0$). Matching these outer solutions as $X \to 0^{\pm}$ to the inner solution (5) as $x \to \pm\infty$ yields the boundary conditions

$$\Phi(0^+, z) = \begin{cases} \Phi(0^+, -z) & \text{for} \quad |z| < (e^2-1)^{\frac{1}{2}} \quad (6a) \\ \Phi(0^-, Z) & \text{for} \quad (e^2-1)^{\frac{1}{2}} \leqslant |z| \leqslant e \quad (6b) \end{cases}$$

on the outer solutions, where

$$Z = \operatorname{sgn}(z)\,(z^2 + 1 - e^2)^{\frac{1}{2}}$$

and $O(E^{\frac{1}{2}})$ terms are neglected.

The outer variables satisfying the governing equations (1) and the $O(1)$ Ekman conditions (3) are

$$u = \partial\Phi/\partial z, \quad v = g, \quad w = -\partial\Phi/\partial X, \tag{7}$$

where Φ and g are integration functions of X and z. Here u and Φ denote $O(1)$ terms and v and w denote $O(E^{\frac{1}{2}})$ terms, these being the leading terms in the asymptotic expansions for these variables in both pipes (see § 6).

The $O(E^{\frac{1}{2}})$ Ekman condition needed to determine Φ and g is derived as follows. Equations (1) are written in cylindrical co-ordinates (r, θ, x), where the y axis lies in the plane $\theta = 0$ and the z axis lies in the plane $\theta = \frac{1}{2}\pi$. The x scale is compressed as before and the radial scale is stretched by introducing

$$n = E^{-\frac{1}{2}}(f - r),$$

where now

$$f = \begin{cases} 1 & \text{for} \quad X < 0, \\ e & \text{for} \quad X > 0. \end{cases}$$

The $O(1)$ Ekman-layer variables, denoted by capitals, which satisfy the resulting equations and match the $O(1)$ axial core velocity $v_x(r, \theta, x)$ are

$$V_x = v_x(f, \theta, x)\,[1 - \cos(\alpha n)\exp(-\alpha n)],$$

$$V_\theta = -\operatorname{sgn}(\cos\theta)\, v_x(f, \theta, x)\sin(\alpha n)\exp(-\alpha n),$$

where

$$\alpha = (\tfrac{1}{2}|\cos\theta|)^{\frac{1}{2}}.$$

This solution is substituted into the continuity equation (1a), which is integrated from $n = 0$ to $n = \infty$ to obtain a boundary condition on the $O(E^{\frac{1}{2}})$ radial core velocity:

$$v_r = -\operatorname{sgn}(\cos\theta)\,(\tan\theta v_x + 2\partial v_x/\partial\theta)/4\alpha f \quad \text{at} \quad r = f.$$

This represents nothing more than the familiar Ekman pumping.

In order for the solution (7) to satisfy this additional Ekman condition, g must be zero and Φ must satisfy

$$(f^2 - z^2)\,\partial^2\Phi/\partial z^2 + \tfrac{1}{2}z\,\partial\Phi/\partial z = (2/f)^{\frac{1}{2}}z(f^2 - z^2)^{\frac{3}{4}}\,\partial\Phi/\partial X. \tag{8}$$

The solution of (8) must also satisfy the regularity conditions (4), which now become

$$(f^2 - z^2)^{-\frac{1}{4}}\,\partial\Phi/\partial z \to 0 \quad \text{as} \quad z \to \pm f. \tag{9}$$

For fully developed flow in an infinite pipe

$$f = 1, \quad \partial\Phi/\partial X = -c_1, \quad \text{a constant},$$

so that the solution of (8) and (9) is

$$\Phi = c_1(\Psi(z) - X) + c_2, \tag{10a}$$

where

$$\Psi = 2^{\frac{1}{2}}\int_0^z (1 - t^2)^{\frac{3}{4}}\,dt, \tag{10b}$$

c_2 is an additive constant pressure and c_1 is determined by the mass-flux condition (2b):

$$c_1 = 2{\cdot}1\,(\tfrac{1}{2}\pi)^{\frac{1}{2}}\,\Gamma(\tfrac{3}{4})/\Gamma(\tfrac{1}{4}) = 0{\cdot}890. \tag{10c}$$

If this solution is rescaled so that $u = 1$ at $z = 0$ and $f = 0{\cdot}5$, it is then identical to the solution given by Benton & Boyer (1966), which agrees well with their experimental results.

Separation of the variables according to

$$\Phi = \psi(\zeta)\exp(\lambda X f^{-2}2^{-\frac{1}{2}}), \quad \zeta = zf^{-1}, \tag{11}$$

reduces (8) and (9) to an eigenvalue problem governed by the ordinary differential equation

$$(1-\zeta^2)\psi'' + \tfrac{1}{2}\zeta\psi' = \lambda\zeta(1-\zeta^2)^{\frac{3}{4}}\psi \tag{12}$$

in $-1 < \zeta < 1$, together with the conditions

$$(1-\zeta^2)^{-\frac{1}{4}}\psi' \to 0 \quad \text{as} \quad \zeta \to \pm 1. \tag{13}$$

The constant f has now disappeared, so that the eigenfunctions and eigenvalues apply to a pipe of any diameter and in particular to both the upstream and downstream pipes.

In general, the eigenvalues of the problem (12) and (13) occur in pairs $\lambda_{\pm j}$ ($j = 1, 2, 3, \ldots$), where $\lambda_{-j} = -\lambda_j < 0$ and $\psi_{-j}(\zeta) = \psi_j(-\zeta)$. The exception is $\lambda_0 = 0$, which is a double eigenvalue, corresponding to fully developed flow. The two eigenfunctions for λ_0 correspond to c_1 and c_2 in the solution (10).

Equation (12) is a Sturm–Liouville equation with a weighting function

$$q(\zeta) = \zeta(1-\zeta^2)^{-\frac{1}{2}},$$

and the conditions (13) are precisely the ones needed to prove the orthogonality of the eigenfunctions (see Courant & Hilbert 1953, p. 291). Thus the eigenfunctions for $\lambda_{\pm j} \neq 0$ are orthogonal to each other and to both eigenfunctions for $\lambda_0 = 0$:

$$\int_{-1}^{1} q\psi_i\psi_k\,d\zeta = 0 \quad \text{for} \quad i, k \neq 0, \quad i \neq k,$$

$$\int_{-1}^{1} q\psi_i\,d\zeta = \int_{-1}^{1} q\psi_i\Psi\,d\zeta = 0 \quad \text{for} \quad i \neq 0.$$

The negative eigenvalues λ_{-j} are excluded upstream and the positive eigenvalues λ_j excluded downstream because they make Φ unbounded as $X \to \mp\infty$ respectively. The solution in each pipe can be expanded in the remaining eigenfunctions, the coefficients in the two expansions being determined by the boundary conditions (6). A numerical scheme for this purpose is presented in the next section.

4. Numerical analysis

Each eigenvalue is found by adjusting λ until a fourth-order Runge–Kutta integration of (12) yields a ψ which satisfies both regularity conditions (13).

The fractional power in (12) makes it difficult to investigate the solution near $\zeta = \pm 1$. With the substitutions

$$\psi(\zeta) = h(\xi), \quad \zeta = 1-\xi^4 \quad \text{for} \quad 0 \leqslant \zeta \leqslant 1,$$

equation (12) becomes

$$\xi(2-\xi^4)h'' - (8-5\xi^4)h' = 16\lambda\xi^6(1-\xi^4)(2-\xi^4)^{\frac{3}{4}}h \tag{14}$$

in $0 \leqslant \xi \leqslant 1$, and the condition (13) at $\zeta = 1$ becomes

$$\xi^{-4}h' \to 0 \quad \text{as} \quad \xi \to 0. \tag{15}$$

The coefficient of h'' in (14) vanishes at $\xi = 0$, so a power series in ξ is used to find the values of h and h' at ξ_0, where $0 < \xi_0 \ll 1$, the numerical integration taking over at ξ_0. Substituting

$$h = \xi^\beta \left(1 + \sum_{j=1}^{\infty} A_j \xi^j\right) \tag{16}$$

into (14) yields a quadratic equation for β with roots $\beta = 0$ and 5, as well as recursion formulae for the coefficients A_j in each case. The first root satisfies the condition (15) because the first six corresponding coefficients A_j for

$$j = 1, 2, \ldots, 6$$

are all zero, while the second root is excluded by condition (15).

For the present calculations, the series (16), with $\beta = 0$, was truncated after 25 terms and was used to obtain h and h' at $\xi_0 = 0{\cdot}001$ for a given value

$$\lambda = \Lambda > 0.$$

A fourth-order Runge–Kutta integration of (14) from ξ_0 to 1 with a step size of 0·001 was used to obtain the values of h and h' at $\xi = 1$.

With the substitutions

$$\psi(\zeta) = H(\xi), \quad \zeta = \xi^4 - 1 \quad \text{for} \quad -1 \leqslant \zeta \leqslant 0,$$

equation (12) and condition (13) at $\zeta = -1$ become equation (14) and condition (15) with h replaced by H and λ by $-\lambda$. Thus the procedure just outlined for $0 \leqslant \zeta \leqslant 1$ is repeated with $\lambda = -\Lambda$ to obtain the values of H and H' at $\zeta = 1$. The trial value $\lambda = \Lambda$ is an eigenvalue if

$$\Delta = h(1)\,H'(1) + h'(1)\,H(1)$$

is zero. If the 'error' Δ turns out to be non-zero, λ must be adjusted and the procedure repeated until Δ vanishes.

First Δ was computed for a range of values $\lambda = 50, 100, 150, 200, \ldots$, in order to locate all the eigenvalues by changes in sign. Then the eigenvalue in any particular interval of λ was determined by repeated linear interpolation, four or five iterations giving eight-place accuracy. The first 36 positive eigenvalues are listed in table 1. The second difference of adjacent eigenvalues is approximately 35·6 throughout, indicating that none have been missed. The corresponding eigenfunctions ψ_j are of no particular interest and are not given here.

The outer solutions in the upstream and downstream pipes are now approximated by the truncated eigenfunction expansions

$$\left.\begin{aligned} \Phi &= c_1(\Psi(z) - X) + \sum_{i=1}^{36} a_i \psi_i(z) \exp(\lambda_i X 2^{-\frac{1}{2}}), \\ \Phi &= c_1 e^{-1}(\Psi(ze^{-1}) - Xe^{-2}) + b_0 + \sum_{L=1}^{36} b_i \psi_i(-ze^{-1}) \exp(-\lambda_i X e^{-2} 2^{-\frac{1}{2}}), \end{aligned}\right\} \tag{17}$$

23·61	1831·62	6522·92	14097·76
82·13	2210·49	7222·17	15117·42
176·25	2624·95	7957·01	16172·69
305·94	3075·01	8727·46	17263·57
471·24	3560·67	9533·50	18390·05
672·12	4081·92	10375·15	19552·15
908·60	4638·77	11252·40	20749·85
1180·68	5231·22	12165·25	21983·17
1488·35	5859·27	13113·70	23252·11

TABLE 1. First 36 positive eigenvalues

respectively. Here the leading terms represent fully developed flow (10), corresponding to $\lambda_0 = 0$, which has been normalized to give a mass flux of π in both pipes. An unnecessary additive constant in the upstream solution has been dropped.

The 73 coefficients a_i, b_0 and b_i for $i = 1, 2, 3, \ldots, 36$ are determined as follows. First the expansions (17) are substituted into the boundary conditions (6). Next (6*b*), which defines $\Phi(0^-, Z)$ for $-1 \leqslant Z \leqslant 1$, is multiplied by $q(Z)\psi_j(Z)$ for $j = 1, 2, 3, \ldots, 36$ and integrated over this Z range to obtain 36 linear algebraic equations. Similarly, equations (6), which together define $\Phi(0^+, z)$ for

$$-e \leqslant z \leqslant e,$$

are multiplied by $q(ze^{-1})\psi_j(-ze^{-1})$ for $j = 1, 2, 3, \ldots, 36$ and by $q(ze^{-1})\Psi(ze^{-1})$, the resulting equations being integrated over this z range to obtain 37 more equations. Finally these 73 equations are solved to obtain the 73 coefficients in the expansions (17).

Once the outer solutions for Φ in both pipes are known, the corresponding velocities are given by (7), the unknown function $\Phi(s)$ in the inner solution is obtained by matching this solution and the downstream outer solution, and the velocities in the expansion are given by (5).

For the present calculations, the eigenfunctions were normalized by

$$\psi_j(-1) = \lambda_j^{-4}$$

because the values 1 and λ_j^{-2} led to integrals which were too large for the computer. Simpson's rule was used to evaluate the integrals of products of eigenfunctions which appear as coefficients in the equations governing a_i, b_0 and b_i.

5. Results and discussions for $e = 1{\cdot}5$

Several profiles of Φ for the upstream and downstream outer solutions are presented in figure 4 for an expansion with $e = 1{\cdot}5$. Equations (7), with $v = 0$, imply that Φ is a stream function for the velocity in the outer solutions, so the surfaces $\Phi =$ constant are stream surfaces, just as they are in geostrophic flow, although they no longer coincide with the geostrophic surfaces. The streamlines $\Phi = -1{\cdot}0, -0{\cdot}8, -0{\cdot}6, \ldots, 1{\cdot}2$ in the $y = 0$ plane are plotted in figure 5. It should

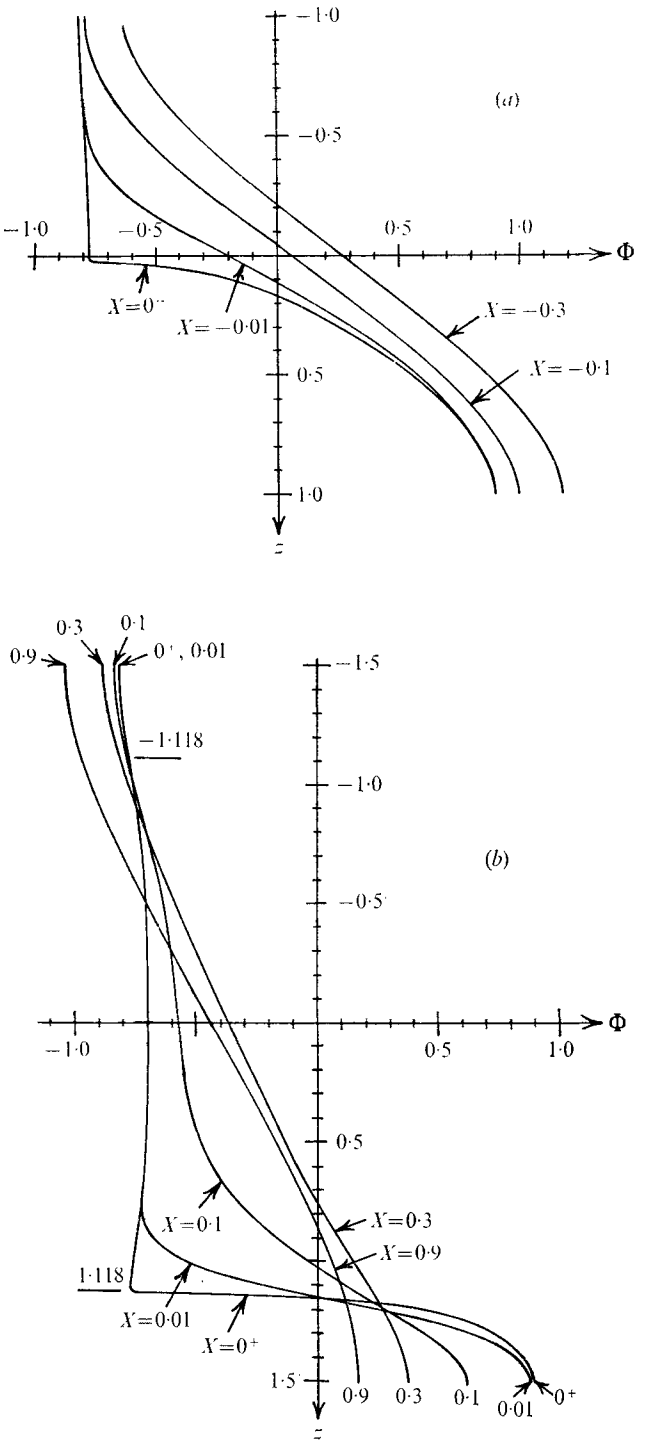

FIGURE 4. Profiles of Φ for $e = 1{\cdot}5$ in the (a) upstream and (b) downstream pipes.

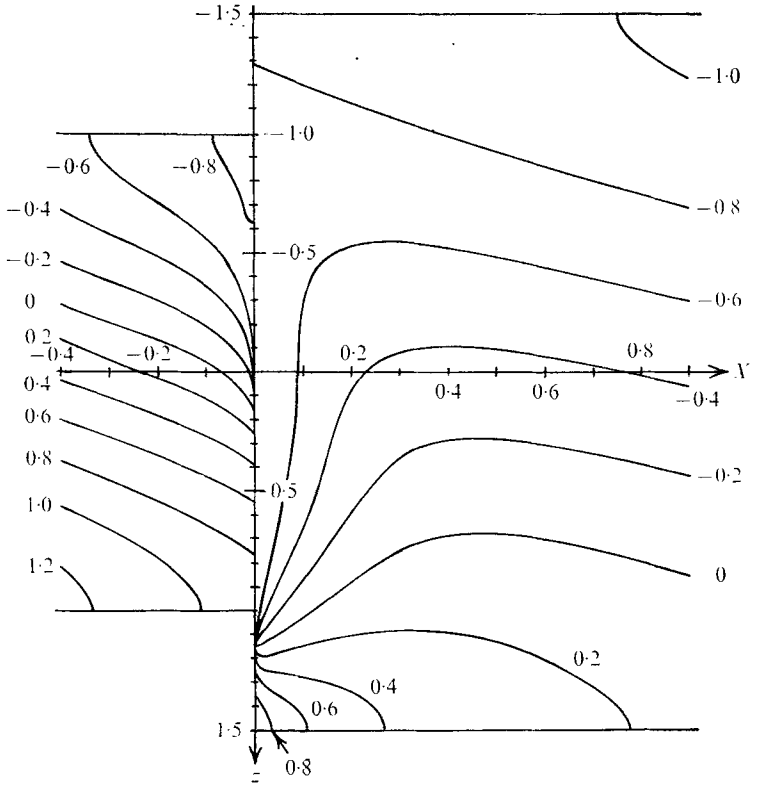

FIGURE 5. Streamlines $\Phi = -1{\cdot}0, -0{\cdot}8, -0{\cdot}6, \ldots, 1{\cdot}2$ in the plane $y = 0$.

be remembered that X is a compressed x scale, so that the streamline slopes are greatly exaggerated.

Upstream the flow is drawn in the $+z$ direction and the streamlines for $-0{\cdot}775 < \Phi < 0{\cdot}4$ are concentrated in the interval $0 < z < 0{\cdot}4$ at $X = 0^-$. These streamlines follow the geostrophic surfaces $0{\cdot}84 < s < 1$ inside the expansion and enter the downstream pipe in the interval $(e^2-1)^{\frac{1}{2}} = 1{\cdot}118 < z < 1{\cdot}2$. They fan out in the downstream pipe, so that fully developed flow is re-established in a relatively short distance on the X scale.

The streamlines $\Phi = -0{\cdot}78, -0{\cdot}76, -0{\cdot}74, \ldots, -0{\cdot}60$ in the plane $y = 0$ for $0 < X < 0{\cdot}08$ are plotted in figure 6. All of these streamlines except $\Phi = -0{\cdot}78$ are concentrated in $1{\cdot}118 < z < 1{\cdot}135$ at $X = 0^+$. For $-0{\cdot}775 < \Phi < -0{\cdot}698$, the streamlines bend backwards, so $u < 0$, and return to $X = 0^+$ in $0 < z < 1{\cdot}118$. They follow the geostrophic surfaces $1 < s < 1{\cdot}5$ inside the expansion and cross $X = 0^+$ a third time in $-1{\cdot}118 < z < 0$. For $-0{\cdot}698 < \Phi < -0{\cdot}625$, the streamlines also bend backwards, so $u < 0$, but bend forwards again without returning to $X = 0^+$. For $\Phi < -0{\cdot}775$ and $\Phi > -0{\cdot}625$, u is always positive.

The approach to fully developed flow upstream and downstream is illustrated by plots of the values of Φ and u on the centre-plane $z = 0$, which are given in figure 7. Figures 7 (*a*) and (*b*) indicate that the flow begins to deviate from fully

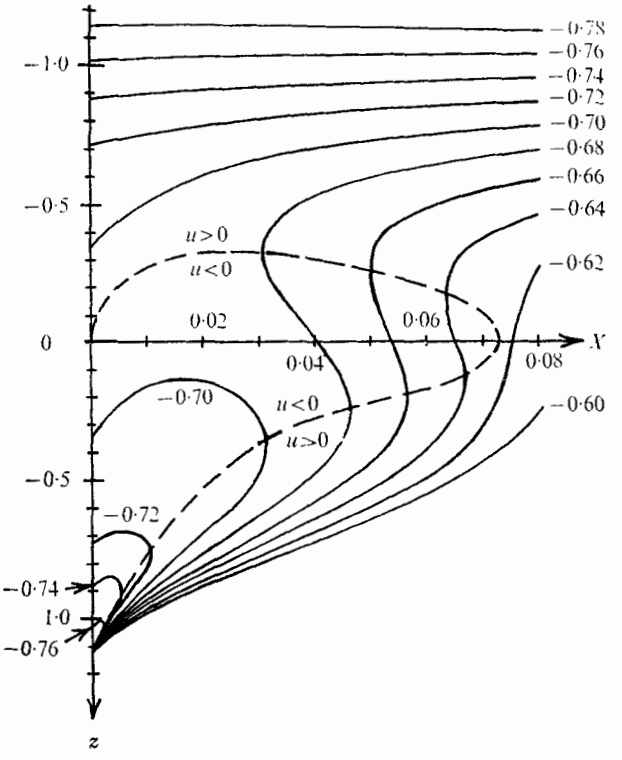

FIGURE 6. Streamlines $\Phi = -0{\cdot}78, -0{\cdot}76, -0{\cdot}74, \ldots, -0{\cdot}60$ in the plane $y = 0$ for $0 < X < 0{\cdot}08$.

developed flow at $X = -0{\cdot}25$, while figures 7(*c*) and (*d*) indicate that the flow returns to fully developed flow at $X = 0{\cdot}9$.

In the solution for $e = 1{\cdot}5$, $b_0 = -0{\cdot}19926$ (the values of a_i and b_i for $i = 1, 2, 3, \ldots, 36$ are of no particular interest). If a geostrophic flow could match both fully developed flows, b_0 would be zero, so b_0 represents the pressure drop required to effect the complicated transition from one fully developed flow to the other.

One rather interesting result is that the flow in both pipes is independent of the shape f and length l of the expansion and depends only on the expansion ratio e. The analysis also shows quite generally that entrance and exit effects persist for a large, $O(E^{-\frac{1}{2}})$ distance into rapidly rotating pipes, which means that fully developed flow will almost never be realized in practice. Part of the difference between fully developed flow and the experimental results obtained by Benton & Boyer (1966) may very well be due to entrance and exit effects, since $100 < E^{-\frac{1}{2}} < 149$ for their experiments. Their tentative conclusion that this difference might decrease if Ro and E were reduced may not be true in view of the present results.

The analysis for circular expansions can be extended to rapidly rotating expansions with other cross-sections provided that no segment of the wall is parallel to the axis of rotation. In fact, the general discussion given by Walker

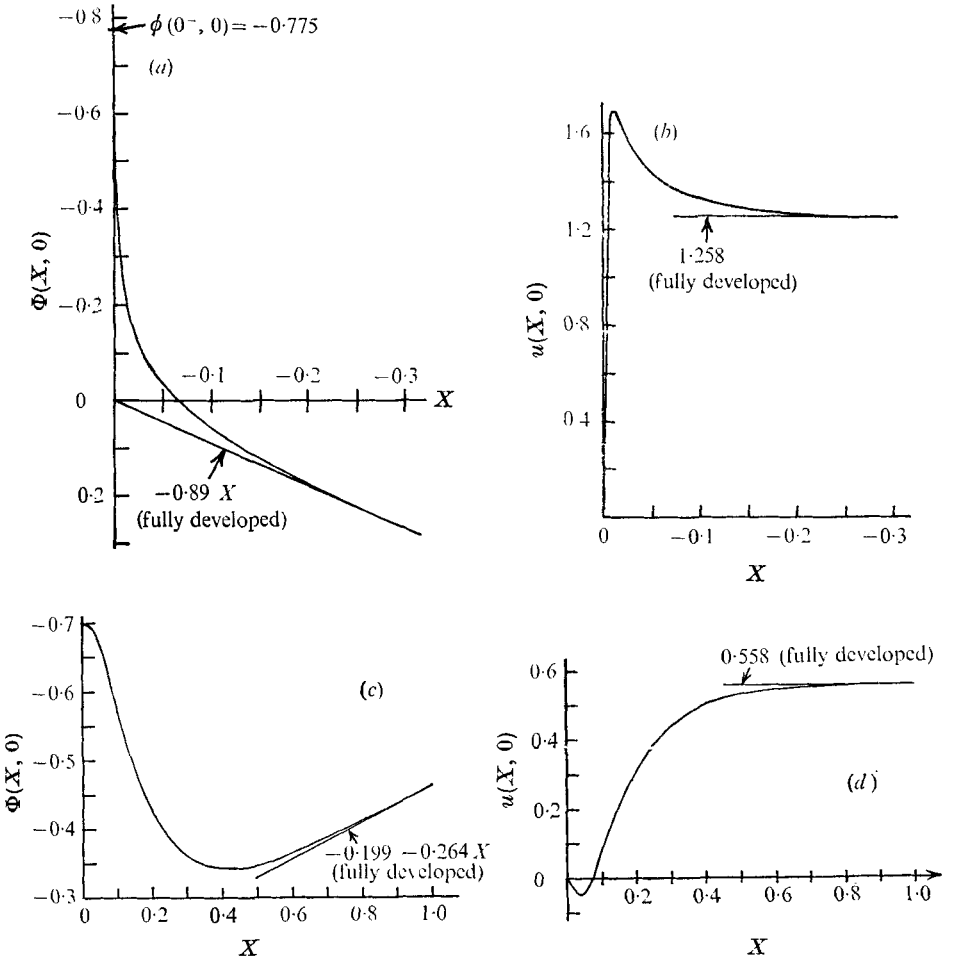

FIGURE 7. Values of Φ and u at $z = 0$, showing the approach to fully developed flow. (*a*) Φ and (*b*) u in the upstream pipe. (*c*) Φ and (*d*) u in the downstream pipe.

& Ludford (1974) for MHD flow in insulated circular expansions applies here. Finally, this analysis coupled with that for rapidly rotating rectangular expansions (Walker 1975) also covers expansions with wall segments parallel to the axis of rotation. With this extension, solutions are known for all rapidly rotating expansions.

6. Limitations of the inertialess approximation

The governing equations (1) involve two parameters, so the asymptotic analysis in each subregion of the flow involves a double power series in Ro and E for each variable. For the core inside the expansion $(\mathbf{v}.\nabla)\mathbf{v}$ is $O(1)$, so that the correct expansion for Φ is

$$\Phi = \sum_{i=0}^{\infty} \sum_{j=0}^{\infty} Ro^i E^{\frac{1}{2}j} \Phi^{(i,j)}, \tag{18}$$

where the coefficient functions are independent of Ro and E. The other expansions are identical. The variables in (5) actually represent $\Phi^{(0,0)}$, $u^{(0,0)}$, $v^{(0,0)}$ and $w^{(0,0)}$. The present analysis uses only the leading terms, so the only restriction on Ro is

$$Ro \ll 1. \tag{19}$$

The Reynolds number $Re = Ud/\nu = Ro/E$, so condition (19) is equivalent to

$$Re \ll E^{-1},$$

which is the condition given by Benton & Boyer (1966).

For the core in the two pipes $(\mathbf{v}.\nabla)\mathbf{v}$ is $O(E^{\frac{1}{2}})$ so the correct asymptotic expansion for Φ (or u) is still (18), while the correct one for v (or w) is

$$v = E^{\frac{1}{2}} \sum_{i=0}^{\infty} \sum_{j=0}^{\infty} Ro^i E^{\frac{1}{2}j} v^{(i,j)}.$$

The variables in (7) actually denote $\Phi^{(0,0)}$, $u^{(0,0)}$, $v^{(0,0)}$ and $w^{(0,0)}$ in these asymptotic expansions. Again only leading terms are needed and the restriction (19) suffices.

Consideration of the Ekman layers and side regions inside the expansion and in the two pipes yields the same condition (19) on Ro.

Since separation is intrinsically inertial, it is suppressed in the inertialess approximation.

If f is continuous but f' is not, a free shear layer $O(E^{\frac{1}{3}})$ in thickness occurs at the cross-section where f' is discontinuous. The flow upstream and downstream is geostrophic, the normal velocity is continuous across the layer and the layer accommodates the jump in tangential velocity. The analysis of such a layer involves $O(E^{\frac{1}{3}})$ terms in (1b) while $(\mathbf{v}.\nabla)\mathbf{v}$ is $O(E^{-\frac{1}{3}})$, so that the inertialess approximation requires

$$Ro \ll E^{\frac{2}{3}}.$$

Combining the present analysis with that for $O(E^{\frac{1}{3}})$ layers (Howard 1969, p. 93) yields the inertialess solution for a conical expansion placed between two pipes, for example.

If f itself is discontinuous, the flow is much more complex and it does not appear to be inertialess in the neighbourhood of the discontinuity no matter what restrictions are placed on Ro. It seems likely that separation would occur in a sudden expansion or contraction no matter how fast the speed of rotation.

The author is deeply indebted to Dr J. C. R. Hunt and Dr G. S. S. Ludford for arousing his interest in the present problem. This research was supported by the National Science Foundation under Grant GK 37427.

REFERENCES

Benton, G. S. & Boyer, D. 1966 Flow through a rapidly rotating conduit of arbitrary cross-section. *J. Fluid Mech.* **26**, 69–79.

Courant, R. & Hilbert, D. 1953 *Methods of Mathematical Physics.* Interscience.

Greenspan, H. P. 1968 *The Theory of Rotating Fluids.* Cambridge University Press.

HOWARD, L. N. 1969 *Rotating Flow.* Lectures at the Royal Institute of Technology, Stockholm.

STEWARTSON, K. 1966 On almost rigid rotations. Part 2. *J. Fluid Mech.* **26**, 131–144.

WALKER, J. S. 1975 Steady flow in rapidly rotating rectangular expansions. To appear in *J. Fluid Mech.*

WALKER, J. S. & LUDFORD, G. S. S. 1974 MHD flow in insulated circular expansions with strong transverse magnetic fields. To appear in *Int. J. Engng Sci.*